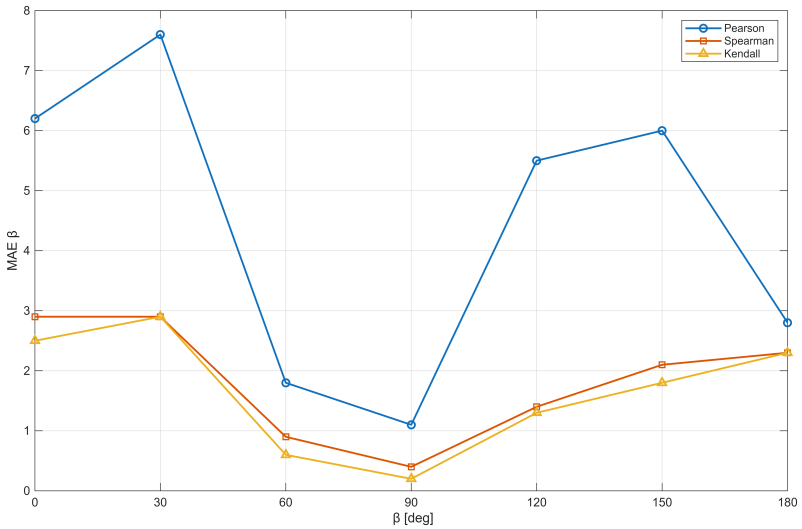

(a) Assessment of main wave direction by Pearson, Spearman and Kendall correlation coefficients – Time interval 60 min

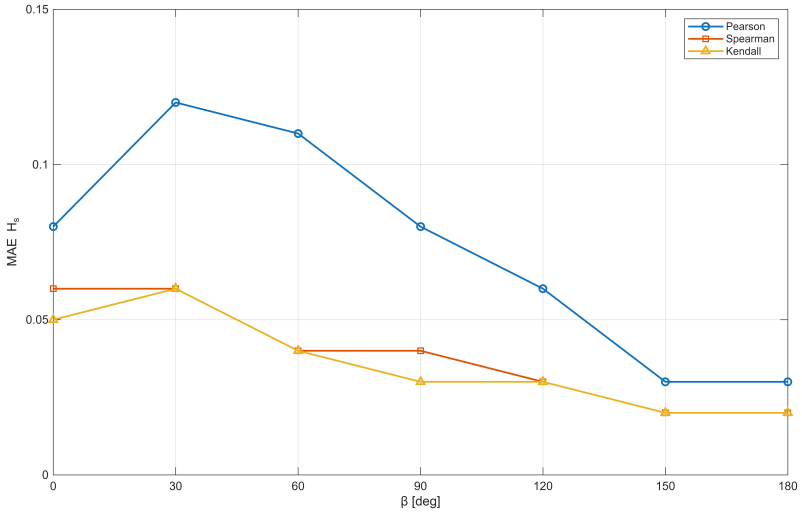

(b) Assessment of significant high wave by Pearson, Spearman and Kendall correlation coefficients – Time interval 60 min

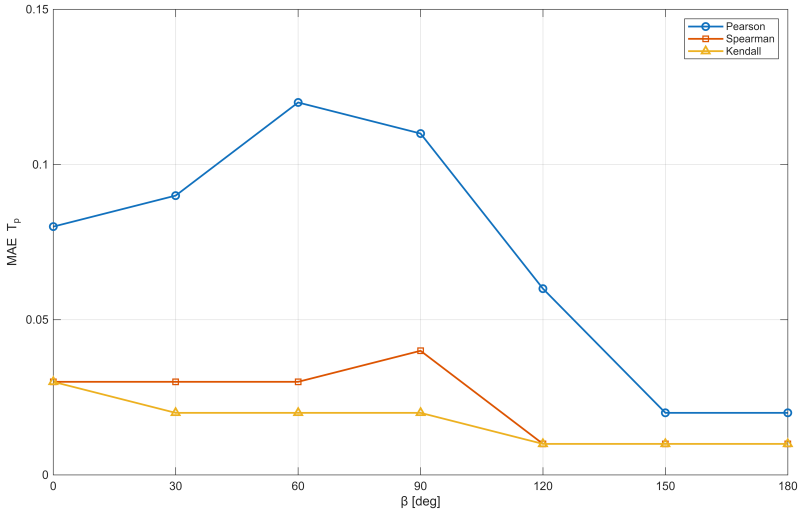

(c) Assessment of wave peak period by Pearson, Spearman and Kendall correlation coefficients – Time interval 60 min

Figure 6.7: Assessment of the main wave parameters by Pearson, Spearman and Kendall correlation coefficients

Dimension	Value	Unit
Length between perpendiculars	232.0	m
Breadth	32.2	m
Design draught	10.8	m
Block coefficient	0.685	-
Deadweight	40,900	t

Table 6.9: Main dimensions of the reference ship.

The vessel was equipped with three types of measurement systems:

- a six DOF Motion Response Unit (MRU), located close to the vessel centre of gravity and coupled with a set of accelerometers, installed in the bosun store close to the ship forward perpendicular;
- a GNSS receiver, installed to acquire the vessel position and speed;
- a wave radar device, namely the Wavex® by Miros.

The ship motion dataset was collected over a four-year span, but the onboard wave radar was installed in September 2007. Therefore, the measurements refer to September 2007 to March 2009, when the vessel was employed in a commercial trade in the Atlantic Ocean (Storhaug, 2007). The vessel operated on almost the same routes, from Western Europe to Canada and viceversa, as shown in Figure 6.8, where the black dots indicate the vessel positions, while the vertical red dashed lines define the boundaries of the open sea region, where the algorithm has been tested. Measurements outside these boundaries were discarded due to the proximity to coastal areas and possible route variations.

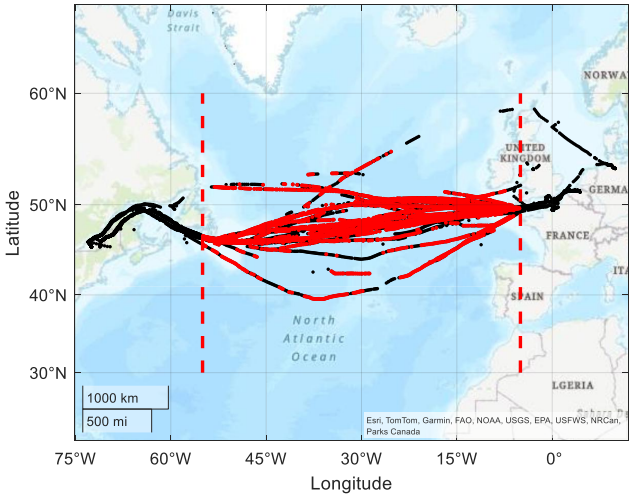

Figure 6.8: Analysed time series (red dots) and original data set (black dots).

The Wasim 3*D* panel code was employed to compute the ship transfer functions at the design draught for 5 reference ship speeds, ranging from 17 to 21 kns. By applying a 0.5 kn tolerance, only measurements within the interval from 16.5 to 21.5 kn were employed in the benchmark study. Each time series was 1500 sec long, with a 5 Hz sampling frequency. Additionally, non-stationary time series that failed the linearity check, based on the Husid function (Gledić et al., 2022), were excluded by Equation 6.7:

$$H_{ui}(t) = \int_0^t a_i^2(\tau)d\tau \tag{6.7}$$

with $0 \leq t \leq T_d$ and having denoted by T_d the time interval.
After applying these restrictions, the time series was reduced from 7645 to 3178.
The estimated significant wave height, the wave peak period and the compass angle of the prevailing wave direction are compared with the relevant values provided by the onboard wave radar, considered as the ground truth, and the ERA5 dataset, released by the European Centre for Medium-Range Weather Forecasts. In this respect, Figure 6.9 provides a comparative analysis between the sea state reconstruction algorithm and the wave radar and ERA5 dataset, with reference to the significant wave height, the wave peak period and the compass angle. In addition, Figure 6.10 depicts the Absolute Errors on the estimated sea state parameters in correspondence of the recoded vessel position. Green, yellow and red dots correspond to AEs on significant wave height and wave peak period less than 35%, greater than 35% and less than 50% and greater than 50%, respectively. Similar threshold values in degs are selected for the Absolute Errors on the compass angle. By Figure 6.10, it is gathered that most of the absolute errors correspond to green dots, confirming the reliability of the wave buoy analogy methods as regards other measurements systems.

An additional investigation was performed considering the geographical area where the ship was sailing and the simultaneous presence of swell conditions that superimpose to the wind sea ones. Indeed, wide ocean regions, apart from some areas of the North Atlantic, the Baltic Sea, the southern North Sea and the Aegean Sea, are highly swell-dominated, which implies that sea spectra are generally double-peaked and the assumption of unimodal sea state conditions is no more valid. In this respect, a classification of sea state conditions crossed by the ship along its route was provided. The ERA5 dataset of wind and swell significant wave height was downloaded for the investigated period from September 2007 to March 2009. These data were used to assess the probability that the investigated geographical area was dominated by either unimodal or bimodal sea state conditions, according to Equation 6.8.

$$E^S(x, y, t) = \frac{H_S^2(x, y, t)}{H_W^2(x, y, t) + H_S^2(x, y, t)} \tag{6.8}$$

The probability evaluated at each grid point *x,y* is defined as the frequency of occurrence of

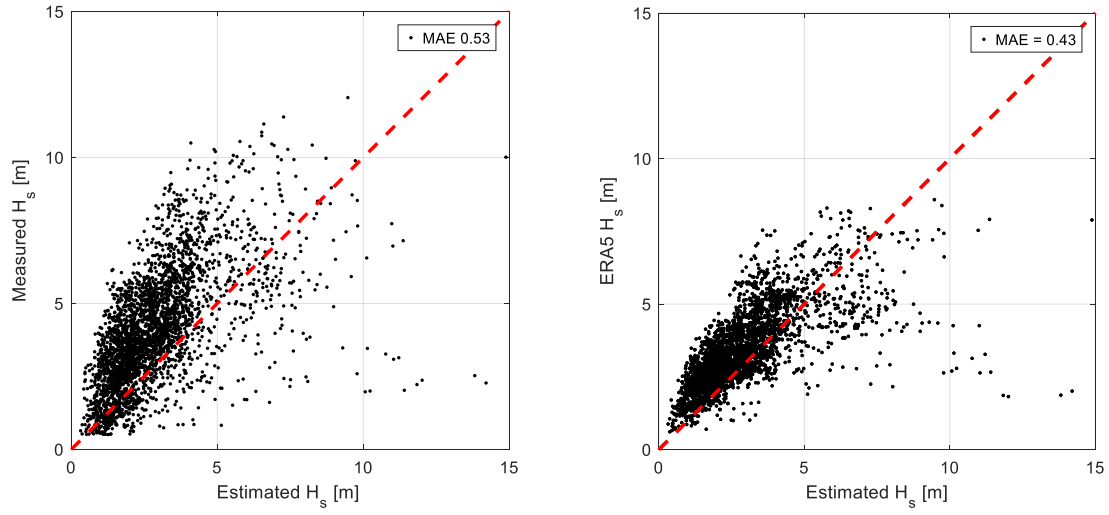

(a) Significant wave height – wave radar

(b) Significant wave height – ERA5

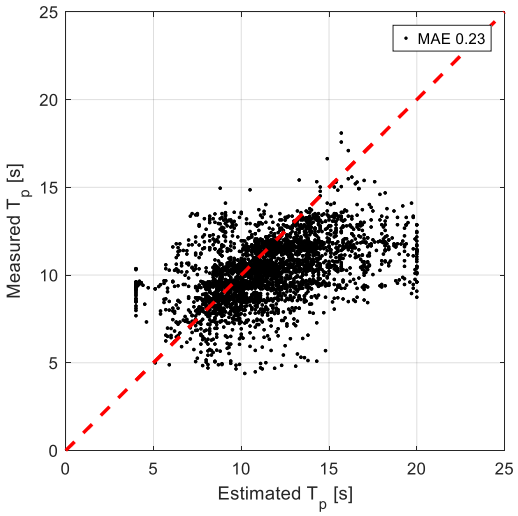

(c) Wave peak period – wave radar

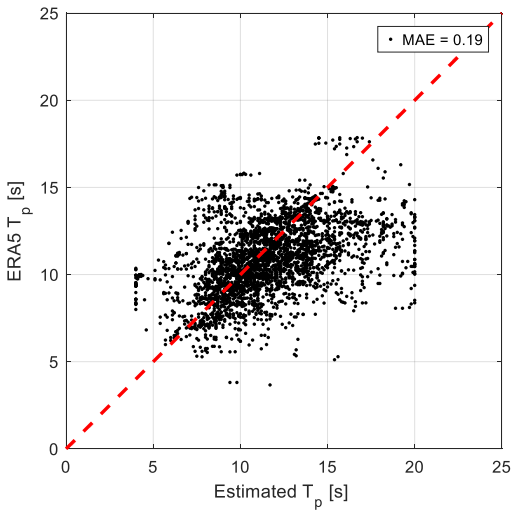

(d) Wave peak period – ERA5

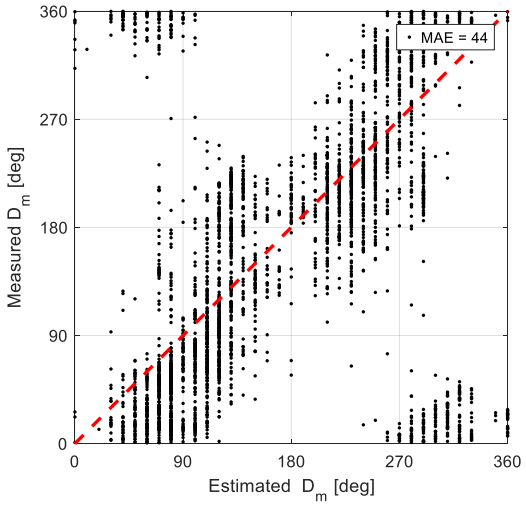

(e) Compass angle – wave radar

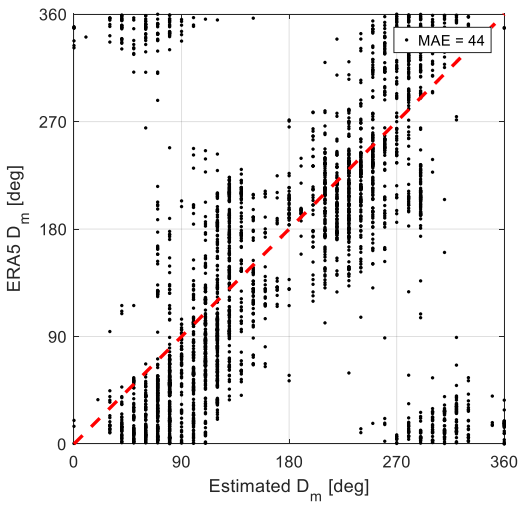

(f) Compass angle – ERA5

Figure 6.9: Comparative analysis of ship motion estimations based on different datasets and evaluation metrics.

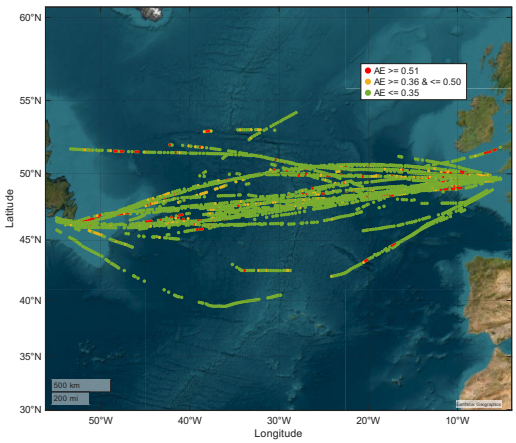

(a) Significant wave height – wave radar

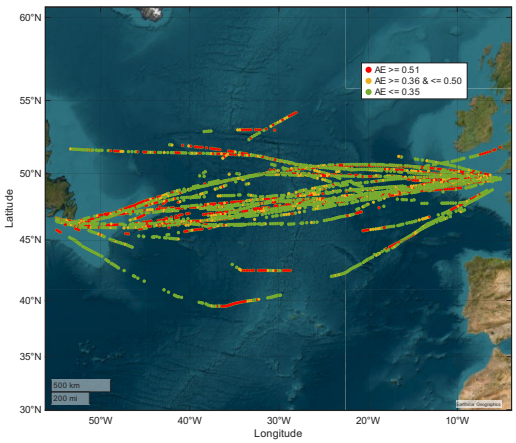

(b) Significant wave height – ERA5

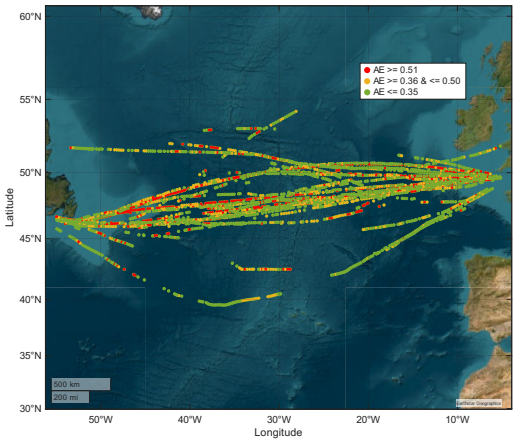

(c) Wave peak period – wave radar

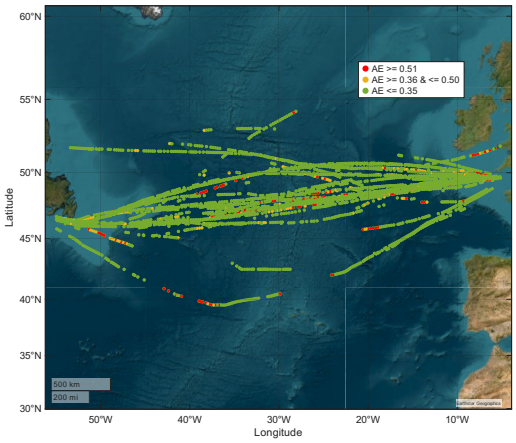

(d) Wave peak period – ERA5

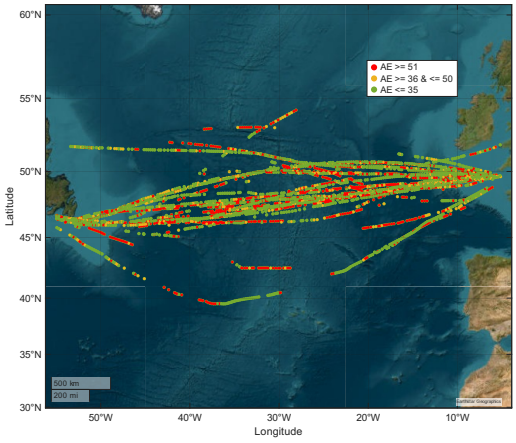

(e) Compass angle – wave radar

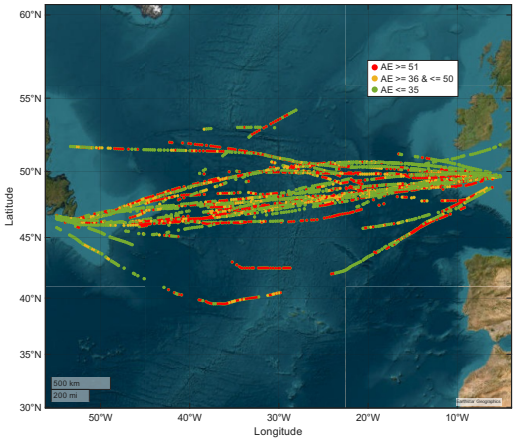

(f) Compass angle – ERA5

Figure 6.10: Comparative analysis of ship motion estimations based on different datasets and evaluation metrics.

a given sea state condition over the total number of available valid observations. The swell energy (E^S) in the spatial and time domain is computed as the ratio of swell significant wave height to the total significant wave one (wind + swell). Based on the E^S value, the sea state is classified as unimodal or bimodal if $E^S \leq 0.15$ or $E^S \geq 0.85$, otherwise, it is classified as bimodal ($0.15 < E^S < 0.85$). In this respect, the maps relative to the spatial distribution of unimodal and bimodal conditions along the ship route are reported in Figure 6.11, where the focus on the North Atlantic area demonstrates that the sea state conditions encountered by the ship are not always unimodal. Based on this consideration, a sensitivity analysis was conducted to evaluate the influence of bimodal sea states. The mean absolute errors (MAE) of the main wave parameters were re-calculated by comparing the ERA5 dataset and the wave radar data in Figure 6.12. The orange histogram bars refer to unimodal sea conditions, while the red bars represent bimodal ones. The MAEs for bimodal sea states are always higher than the unimodal ones. This difference is particularly notable for the significant wave height and the wave peak period. In conclusion, the presence of bimodal seas negatively impacts the estimation of the main wave parameters. Therefore, this outcome further justifies the need of developing sea state reconstruction algorithms for bimodal conditions, as further investigated in Chapter 7.